



# Surface Barrier of Holes Drilled in a Type-II Superconductor

D. M. Gokhfeld<sup>1,2</sup>

Received: 22 March 2023 / Accepted: 9 June 2023 / Published online: 14 June 2023  
© The Author(s), under exclusive licence to Springer Science+Business Media, LLC, part of Springer Nature 2023

## Abstract

Holes drilled in a type-II superconductor trap the magnetic flux. Following Clem's flux pinning model, we consider surface pinning as a mechanism for compressing the magnetic flux in the holes. Estimations of the trapped magnetic flux demonstrate that the holes with the diameter up to 2 mm are advantageous for bulk single-crystal REBCO samples. The REBCO films and tapes can be improved by the holes with diameter smaller than 10  $\mu\text{m}$ .

**Keywords** YBCO · Critical state model · Kim dependence · Clem model · Pinning · Trapped magnetic flux · Perforation

Improving the magnetic and current-carrying properties of superconductors is a crucial and challenging task for sustainable growth [1]. One promising method is perforation, which can enhance oxygenation and prevent cracking in high- $T_c$  samples. Perforation has a direct impact on the magnetic and current-carrying properties [2–7]. Holes can effectively trap magnetic flux [8]. In recent works [9, 10], where a flux trapping was modeled with using the Monte-Carlo method, values of the magnetic field in the holes were fitted to simulate well-defined peaks on the magnetic field profiles. The magnetic field trapped in the holes was 20 times higher than the averaged local field.

In the presented study, the magnetic flux trapped in holes is determined using Clem's surface pinning model [11]. It is proposed that the same barriers for Abrikosov vortices are raised by the superconductor surface and by holes drilled in the superconductor. Perforation parameters for achieving the highest values of trapped magnetic flux are estimated.

Consider a superconducting sample, the long cylinder with the diameter  $D \gg \lambda$ , where  $\lambda$  is the London penetration length. The external magnetic field  $H$  is applied parallel to the main axis of the cylinder, so the demagnetization is negligible. The sample contains holes which are drilled parallel to the main axis. It is assumed that the holes are uniformly distributed over

the end face of the cylinder. The maximum value  $H_{\max}$  of  $H$  is higher than the full penetration field  $H_p$ . The flux  $\Phi$  trapped in the perforated sample after  $H$  decreases to 0 is estimated using the critical state model [12]. Based on the result of the study [10], the following expression is proposed:

$$f = (1 - n_h)(1 + n_h k_h) \quad (1)$$

where dimensionless parameters are used:  $f$  is the reduced trapped flux,  $f = \Phi/\Phi_{\text{pin}0}$ ,  $n_h$  is the perforation coefficient,  $n_h = A_h N_h S_h / S$ , and  $k_h$  is the reduced excess field in the holes,  $k_h = B_h / B_{\text{pin}0}$ . The material-related ( $\Phi_{\text{pin}0}$  is the flux trapped in the unperforated sample,  $B_{\text{pin}0}$  is the corresponding remnant magnetic field,  $B_{\text{pin}0} = \Phi_{\text{pin}0} / S$ , and  $S$  is the area of the sample end face) and the hole-related ( $A_h$  is a coefficient depending on an arrangement of the holes,  $N_h$  is the number of the holes,  $S_h$  is the area of a single hole, and  $B_h$  is the average magnetic field in the holes) parameters are involved. It should be noted that  $A_h$  can be higher than 1 due to perturbations of current trajectories by the holes [10].

The expression (1) allows one to estimate the efficiency of pinning by holes and the perforation parameter for the maximum trapped flux. A condition for the increase of the trapped flux is  $f > 1$ . It is valid for

$$n_h < 1 - \frac{1}{k_h}. \quad (2)$$

The maximum value of trapped flux is

$$f = \frac{1}{4} \left( 2 + k_h + \frac{1}{k_h} \right). \quad (3)$$

✉ D. M. Gokhfeld  
gokhfeld@iph.krasn.ru

<sup>1</sup> Siberian Branch, Kirensky Institute of Physics, Krasnoyarsk Scientific Center, Russian Academy of Sciences, Krasnoyarsk 660036, Russia

<sup>2</sup> Siberian Federal University, Krasnoyarsk 660041, Russia

It is achieved for

$$n_h = \frac{1}{2} \left( 1 - \frac{1}{k_h} \right). \tag{4}$$

Expressions (3–4) were obtained in the previous study [10]. However the value of  $k_h$  was only a varied parameter where. Now we want to relate this parameter to the microscopic parameters of the superconductor. The holes are considered as convoluted surfaces into the superconductor. So an interaction of vortices with the superconducting surface is a subject of interest. The Clem’s surface pinning model [11] considers barriers for Abrikosov vortices appearing and disappearing near a surface of a type-II superconductor. The model statements are the following: i) There is a vortex-free region near the surface; ii) The entry field  $H_{en}$  determines the external field value required for an Abrikosov vortex to nucleate at the surface and move through the vortex-free region; iii) The exit field  $H_{ex}$  needs for an Abrikosov vortex to pass back through the vortex-free region and leave the superconductor. Both  $H_{en}$  and  $H_{ex}$  depend on an averaged magnetic field  $B$  at the inner border of the vortex free region:

$$H_{en} \approx \frac{1}{\mu_0} (B_s^2 + B^2)^{1/2}, \tag{5}$$

$$H_{ex} \approx B/\mu_0,$$

where  $B_s = \Phi_0/(4\pi\lambda\xi)$ ,  $\xi$  is the coherence length,  $\Phi_0 = 2.07 \cdot 10^{-15}$  Wb, and  $\mu_0 = 4\pi \cdot 10^{-7}$  H/m.

We assume that the hole has the similar surface barriers to vortices as the surface, and expression (5) is reliable to describe pinning of vortices in holes. In this case  $H_{en}$  is a maximum value of the magnetic field trapped in the hole. Abrikosov vortices can enter to the holes only if the magnetic field in the hole is not higher than the averaged magnetic field  $B$ . Since  $H_{en} > H_{ex}$ , the holes facilitate the flux propagation but hinder the flux exit. The excess field in the holes is limited by the surface barrier. The reduced excess field is determined by  $k_h \approx [(B_s/B_{pin0})^2 + 1]^{1/2}$ .

Mesoscopic samples may have  $H_p < H_{en}$ . This means that the condition  $H_{max} > H_{en}$  may be wrong for these objects. In this case the magnetic field in the holes equals the average magnetic field in the sample at the external field  $H_{max}$ . One can estimate  $k_h \approx (1/3)\mu_0 H_{max}/B_{pin0}$  for the considered cylindrical geometry.

The holes as well as the sample surface have the vortex-free region around their perimeter. The thickness of this region is not higher than  $\lambda$  [11]. As the vortex-free region affects the reversible magnetization [13, 14], it is expected that the irreversibility field is reduced by perforation.

Any cavities in a type-II superconductor facilitate the propagation of magnetic flux inside. Thus, the perforated

sample has smaller values of the penetration field  $H_p$  and the magnetization width  $\Delta M$  at  $H > H_p$  than those of the unperforated sample. Then the external field is decreased, magnetic flux partially exits from the sample and the averaged magnetic field  $B$  decreases. At the same time the holes prevent the magnetic flux from escaping. As a result, the values of  $\Delta M$  at  $H < H_p$  and the remnant magnetization  $M_{rem} = B_{pin0}/\mu_0$  can be higher for the perforated sample than for the unperforated one. Schematic representations of the magnetization hysteresis loops for perforated and unperforated samples are shown in Fig. 1. The Kim-type dependence  $j_c(B) = j_{c0}/(1 + B/B_1)$  is used to calculate these loops. The perforated sample is appointed to have a higher value of the zero-field critical current density  $j_{c0}$  and a smaller value of the parameter  $B_1$  than the unperforated sample.

Next, the effect of the sample parameters on the trapped flux is analyzed. Let us introduce a material dependent parameter  $b_j = B_{pin0}/B_s$ . Figure 2 demonstrates the  $f(n_h)$  dependence (1) calculated for different values of  $b_j$ . It can be seen that the  $f(n_h)$  dependencies always have a maximum (points marked 1) for the finite values of  $b_j$ , and the maximum position shifts to smaller  $n_h$  for higher  $b_j$ . Positions of  $n_h$  corresponding to pinning advantage  $f > 1$  (points marked 2) have the same behavior. We plot the positions of these points versus the material parameter  $b_j$  (Fig. 3). These plots allow one to choose optimal perforation parameters for known values of  $j_c$  for different superconducting materials.

It appears that the most experimental data of perforated high- $T_c$  samples can be divided into two groups with different  $j_c$ . Bulk REBCO (RE is Y or rare-earth elements) single-crystals have smaller values of  $j_c$ , the typical values are  $j_c \sim 0.001j_d$  at the liquid helium temperature and more than 10 times smaller at liquid nitrogen temperature [7, 15,

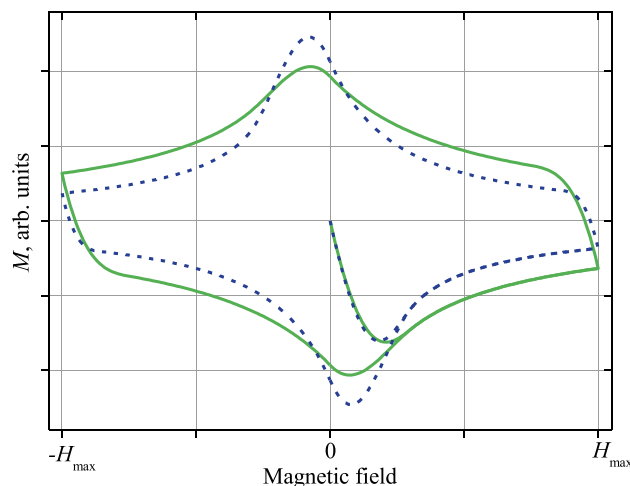
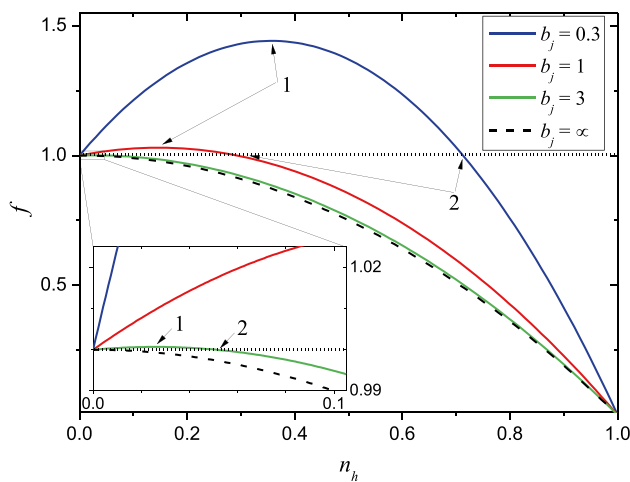


Fig. 1 Schematic representation of magnetization hysteresis loops for an unperforated sample (solid line) and a perforated sample (dashed line)



**Fig. 2** Dependence of trapped flux  $f$  on the perforation coefficient  $n_h$  for different values of  $b_j$ . Inset demonstrates the same  $f(n_h)$  curves at the interval of small  $n_h$ . Arrows indicate 1) the positions of maximal trapped flux and 2) the limiting values of  $n_h$  for  $f > 1$ , i.e. for pinning advantage

16], where  $j_d$  is the depairing current density. REBCO films and tapes have higher values of  $j_c$ , they can have  $j_c \sim 0.1j_d$  at the liquid helium temperature [17, 18].

Using  $B_{pin0} \approx \mu_0 j_c D/6$  for the considered cylinder geometry and given typical parameters of large-grain bulk REBCO samples ( $D = 2$  cm,  $j_c = 10^8$  A/m<sup>2</sup> and  $B_s = 0.17$  T at 77 K), one obtains  $b_j \approx 2.5$ . In this case, the trapped flux enhancement requires  $n_h < 0.07$ . Optimal pinning can be achieved for 15 holes with  $D_h = 1$  mm or for 60 holes with  $D_h = 0.5$  mm. These holes are admitted to be suitable for the refrigerating liquid nitrogen [19]. REBCO tapes with  $j_c \approx 10^{10}$  A/m<sup>2</sup> and  $D = 1$  cm have  $b_j \approx 120$ . This corresponds to  $n_h < 3 \cdot 10^{-5}$  and

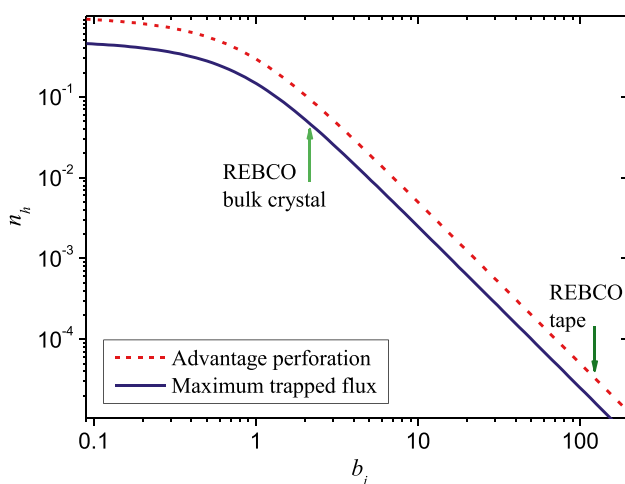


**Fig. 3** The perforation coefficient  $n_h$  providing pinning advantage (dash line) and maximum trapped flux (solid line) versus the material parameter  $b_j$

$D_h < 60$   $\mu$ m. Optimal pinning can be achieved for about 1600 holes with  $D_h = 1$   $\mu$ m or for 16 holes with  $D_h = 10$   $\mu$ m. It is unlikely that liquid nitrogen cooling can be provided by such small diameter holes [20, 21]. A few 100  $\mu$ m diameter holes can be useful for liquid nitrogen cooling [19], but they suppress the trapped magnetic flux. This means that the holes in such REBCO tapes cannot provide the effective cooling and the pinning enhancement at the same time.

In conclusion, the surface barrier created by drilled holes in the superconducting sample is accounted to find the trapped magnetic flux. The influence of perforations on magnetization hysteresis loops of superconductors is also considered. It is expected that perforation will decrease the full penetration field and irreversibility field. However, the remnant magnetization can be increased for a certain range of perforation parameters, and the conditions for this increase are established. Optimal perforation parameters are found for both REBCO bulk single crystals and REBCO tapes.

**Data Availability** The data that support the findings of this study are available from the corresponding author upon reasonable request.

## Declarations

**Conflict of Interest** The author declare no competing interests.

## References

- Muralidhar, M., Srikanth, A.S., Pinmangkorn, S., Santosh, M., Milos, J.: Role of Superconducting Materials in the Endeavor to Stop Climate Change and Reach Sustainable Development. *J. Supercond. Nov. Magn.* 1–10 (2023). <https://doi.org/10.1007/s10948-023-06515-6>
- Bartolomé, E., Granados, X., Puig, T., Obrados, X., Reddy, E.S., Kracunovska, S.: Critical state of YBCO superconductors with artificially patterned holes. *IEEE Trans. Appl. Supercond.* **15**, 2775–2778 (2005). <https://doi.org/10.1109/TASC.2005.848210>
- Lousberg, G.P., Ausloos, M., Vanderbemden, P., Vanderheyden, B.: Bulk high-Tc superconductors with drilled holes: How to arrange the holes to maximize the trapped magnetic flux? *Supercond. Sci. Technol.* **21**, 025010 (2008). <https://doi.org/10.1088/0953-2048/21/02/025010>
- Jang, G., Lee, M., Han, S., Kim, C., Han, Y., Park, B.: Trapped field analysis of a high temperature superconducting bulk with artificial holes. *J. Magn.* **16**, 181–185 (2011). <https://doi.org/10.4283/JMAG.2011.16.2.181>
- Pannetier, M., Wijngaarden, R.J., Fløan, I., Rector, J., Dam, B., Griessen, R., Lahl, P., Wördenweber, R.: Unexpected fourfold symmetry in the resistivity of patterned superconductors. *Phys. Rev. B* **67**, 212501 (2003). <https://doi.org/10.1103/PhysRevB.67.212501>
- Berdiyrov, G.R., Milošević, M.V., Peeters, F.M.: Composite vortex ordering in superconducting films with arrays of blind holes. *New J. Phys.* **11**, 013025 (2009). <https://doi.org/10.1088/1367-2630/11/1/013025>

7. Kuchárová, V., Diko, P., Volochová, D., Antal, V., Lojka, M., Hlášek, T., Plecháček, V.: Microstructure and superconducting properties of bulk EuBCO-Ag with and without holes. *J. Eur. Ceram. Soc.* **42**, 6533–6541 (2022). <https://doi.org/10.1016/j.jeurceramsoc.2022.06.081>
8. Matsumoto, K., Mele, P.: Artificial pinning center technology to enhance vortex pinning in YBCO coated conductors. *Supercond. Sci. Technol.* **23**, 014001 (2010). <https://doi.org/10.1088/0953-2048/23/1/014001>
9. Maksimova, A.N., Kashurnikov, V.A., Moroz, A.N., Gokhfeld, D.M.: Trapped field in superconductors with perforations. *J. Supercond. Nov. Magn.* **35**, 283–290 (2022). <https://doi.org/10.1007/s10948-021-06067-7>
10. Gokhfeld, D.M., Maksimova, A.N., Kashurnikov, V.A., Moroz, A.N.: Optimizing trapped field in superconductors with perforations. *Phys. C Supercond. Appl.* **600**, 1354106 (2022). <https://doi.org/10.1016/j.physc.2022.1354106>
11. Clem, J.R.: A model for flux pinning in superconductors. In: *Low Temperature Physics-LT 13*. pp. 102–106. Springer US, Boston, MA (1974)
12. Bean, C.P.: Magnetization of high-field superconductors. *Rev. Mod. Phys.* **36**, 31–39 (1964). <https://doi.org/10.1103/RevModPhys.36.31>
13. Burlachkov, L., Geshkenbein, V.B., Koshelev, A.E., Larkin, A.I., Vinokur, V.M.: Giant flux creep through surface barriers and the irreversibility line in high-temperature superconductors. *Phys. Rev. B* **50**, 16770–16773 (1994). <https://doi.org/10.1103/PhysRevB.50.16770>
14. Zeng, X.L., Karwoth, T., Koblischka, M.R., Hartmann, U., Gokhfeld, D., Chang, C., Hauet, T.: Analysis of magnetization loops of electrospun nonwoven superconducting fabrics. *Phys. Rev. Mater.* **1**, 044802 (2017). <https://doi.org/10.1103/PhysRevMaterials.1.044802>
15. Lousberg, G.P., Fagnard, J.F., Haanappel, E., Chaud, X., Ausloos, M., Vanderheyden, B., Vanderbemden, P.: Pulsed-field magnetization of drilled bulk high-temperature superconductors: flux front-propagation in the volume and on the surface. *Supercond. Sci. Technol.* **22**, 125026 (2009). <https://doi.org/10.1088/0953-2048/22/12/125026>
16. Li, B., Zhou, D., Xu, K., Hara, S., Tsuzuki, K., Miki, M., Felder, B., Deng, Z., Izumi, M.: Materials process and applications of single grain (RE)–Ba–Cu–O bulk high-temperature superconductors. *Phys. C Supercond. Appl.* **482**, 50–57 (2012). <https://doi.org/10.1016/j.physc.2012.04.026>
17. George, J., Jones, A., Al-Qurainy, M., Fedoseev, S.A., Rosenfeld, A., Pan, A.V.: Tunable pinning effects produced by non-uniform antidot arrays in YBCO thin films. *Ann. Phys.* **529**, 1600283 (2017). <https://doi.org/10.1002/andp.201600283>
18. Pokrovskii, S.V., Mavritskii, O.B., Egorov, A.N., Mineev, N.A., Timofeev, A.A., Rudnev, I.A.: Influence of ultrashort laser drilling on magnetic and transport characteristics of HTS tapes. *Supercond. Sci. Technol.* **32**, 075008 (2019). <https://doi.org/10.1088/1361-6668/ab14a3>
19. Qi, S.L., Zhang, P., Wang, R.Z., Xu, L.X.: Single-phase pressure drop and heat transfer characteristics of turbulent liquid nitrogen flow in micro-tubes. *Int. J. Heat Mass Transf.* **50**, 1993–2001 (2007). <https://doi.org/10.1016/J.IJHEATMASSTRANSFER.2006.09.032>
20. Chung, P.M.Y., Kawaji, M.: The effect of channel diameter on adiabatic two-phase flow characteristics in microchannels. *Int. J. Multiphase Flow* **30**, 735–761 (2004). <https://doi.org/10.1016/J.IJMULTIPHASEFLOW.2004.05.002>
21. Laurent, P., Mathieu, J.P., Mattivi, B., Fagnard, J.F., Meslin, S., Noudem, J.G., Ausloos, M., Cloots, R., Vanderbemden, P.: Study by Hall probe mapping of the trapped flux modification produced by local heating in YBCO HTS bulks for different surface/volume ratios. *Supercond. Sci. Technol.* **18**, 1047–1053 (2005). <https://doi.org/10.1088/0953-2048/18/8/004>

**Publisher's Note** Springer Nature remains neutral with regard to jurisdictional claims in published maps and institutional affiliations.

Springer Nature or its licensor (e.g. a society or other partner) holds exclusive rights to this article under a publishing agreement with the author(s) or other rightsholder(s); author self-archiving of the accepted manuscript version of this article is solely governed by the terms of such publishing agreement and applicable law.